

Supplementary Material: A method for characterizing adsorption of flowing solutes to microfluidic device surfaces

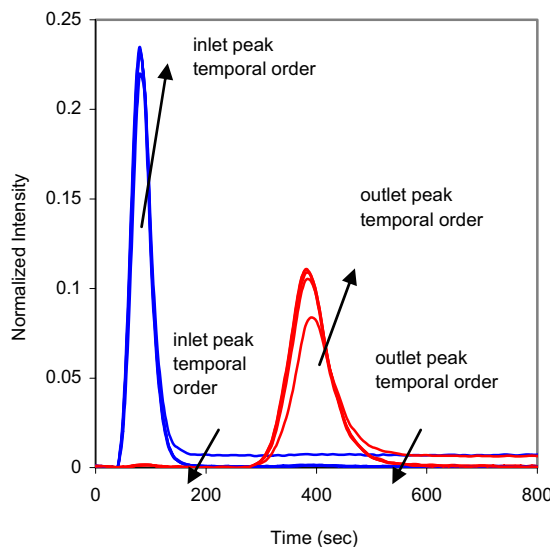
⁵ Kenneth R. Hawkins,*^a Mark R. Steedman,*^b Richard R. Baldwin,^a Elain Fu,^a Sandip Ghosal,^c and Paul Yager^a

Higher concentration FITC-BSA

10 Representative results for FITC-BSA at a higher concentration of 20 μM (Supplementary Material Fig. 1) indicate that the eluted fraction reaches unity after two or three runs, consistent with faster saturation expected from a higher concentration solution (compared to 2 μM FITC-BSA 15 of Figure 3b).

Nonfouling BSA Coating

Representative results for a device that has been pretreated with 20 μM unlabeled BSA and then tested with FITC-BSA 20 show that the trends noted with an untreated device are abolished by the pretreatment step (Supplementary Material Fig. 2). All peaks for this experiment superimpose with good 25 precision.



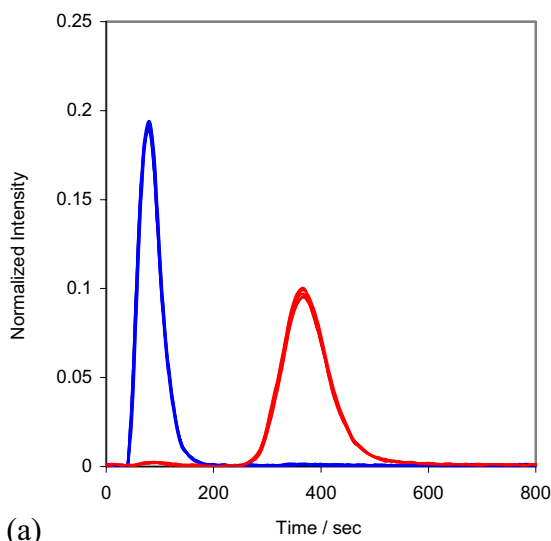
Supplementary Material, Fig. 1 Five representative runs for FITC-BSA at a higher concentration (20 μM). **Blue** lines are observations at the inlet, and **red** lines are observations at the outlet, with the data processing described in the text. A smooth interpolation is used for display. The initial run displays an increased baseline for the inlet and outlet peaks, while subsequent runs are nearly completely resolved.

* khawk@u.washington.edu, mark.steedman@ucsf.edu. These authors contributed equally to the content of this research.

^a Department of Bioengineering, University of Washington, Seattle, Washington, USA. Fax: 1 206.543.3928; Tel: 1 206.543.9374;

^b UCSF/UC Berkeley Joint Graduate Group in Bioengineering, University of California at San Francisco and Berkeley, San Francisco, California, USA Fax: 1 415.476.2414; Tel: 1 415.514.9695;

^c Department of Mechanical Engineering, Northwestern University, Evanston, Illinois, USA. Fax: 1 847.491.3915; Tel: 1 847.467.5990



Supplementary Material, Fig. 2 Five representative runs for FITC-BSA in a device pre-treated with 20 μM unlabeled BSA.). **Blue** lines are observations at the inlet, and **red** lines are observations at the outlet, with the data processing described in the text. A smooth interpolation is used for display. The observed adsorption trend (Fig. 3) is abolished by the pre-treatment.

Simple Predictive Modeling

Perhaps the most meaningful and appropriate negative control is analytical or numerical predictions for peak shape in the absence of adsorption specific to the adsorbant of interest. The usual chromatographer's equations do not apply in many 30 microfluidic situations, and a numerical solution for the temporal evolution of dispersion in arbitrary geometries that accounts for all phenomena requires specialized software and computational power. Therefore, it is useful to determine if simplifying assumptions can be made.

35 Consider the results for fluorescein. Application of the Taylor/Aris equation¹⁻⁴ requires that the solute concentration be almost uniform in the dimensions transverse to flow. For fluorescein in this device, the time-scale of diffusion in the depth dimension is much smaller than the time-scale for advection (the ratio is on the order of 10^{-5}). Thus the Taylor assumption applies in the depth dimension. However,

40 the time-scale for diffusion in the width dimension is about an order of magnitude greater than the time-scale for advection -- the Taylor assumption does not apply in the width dimension.

45 Nevertheless, because of the large aspect ratio of the channel and the small size of the sample window, the velocity profile is close to uniform (in the width dimension) across the sample window. In addition, the advective flux of fluorescein is ~ 1000 times greater than the diffusive flux. Therefore, it seems 50 reasonable to neglect the small transverse fluxes and treat the problem as Taylor dispersion in a slit, with a distance H between the walls.

The theory for flow between parallel plates is well known. The dispersion can be expressed with an effective diffusion coefficient, D_{eff} which is a function of the depth of the channel H , the molecular diffusion coefficient D_m , and the linear velocity U (Supplementary Material Equation 1).

$$D_{\text{eff}} = D_m + \frac{2H^2U^2}{105D_m} \quad (1)$$

Since this system samples the concentration (C) at the centerline of the channel, the correct flow velocity is $3Q/2HW$, where Q is the volumetric flow and W is the channel width⁵.

This effective diffusion coefficient describes the spreading of a delta-function input by $\sigma_d^2=2D_{\text{eff}}$ where σ_d^2 is the peak variance. The variance thus calculated is a parameter in a unity-normalized Gaussian describing the concentration,³ with a centroid (\bar{t}) that is determined by translating the centroid of the input function to a time calculated from the flow velocity and distance between “windows” (Supplementary Material Equation 2).

$$C(t) = \frac{1}{\sqrt{2\pi}\sigma} e^{-\left(\frac{(t-\bar{t})^2}{2\sigma^2}\right)} \quad (2)$$

For arbitrary input functions (ϕ_{in}), the input function must be convoluted with the expected dispersion to correctly describe the outlet peak (ϕ_{out}),³ where $G(t,t')=f(t-t')$ is the Green's function for the one dimensional advection diffusion operator (Supplementary Material Equation 3).

$$\phi_{out}(t) = \int_{-\infty}^{\infty} G(t,t') \phi_{in}(t') dt' \quad (3)$$

The sample injection valve used in this device is assumed to produce a plug of length $\tau = 22.6\text{s}$, which is unity-normalized by the signal processing algorithms. Thus the input function can be written, $C(t')=C_0/\tau$ for $0 \leq t' \leq \tau$. The solution to the integral formed by applying this input to Equation 3 results in a difference of two error functions (Supplementary Material Equation 4), where the variables have the same meaning as in Equation 2, except that the location of the centroid is adjusted by $\tau/2$ to reflect the finite length of the sample plug.³

$$C(t) = \frac{1}{2\tau} \left[\operatorname{erf}\left(\frac{t-\bar{t}}{\sqrt{2}\sigma}\right) - \operatorname{erf}\left(\frac{t-\bar{t}-\tau}{\sqrt{2}\sigma}\right) \right] \quad (4)$$

The error functions in Equation 4 determine the shape of the leading and tailing edges of the peak, and the time displacement of their inflection points determines the duration of any plateau in the peak. With sufficiently short sample pulses, no plateau is expected.

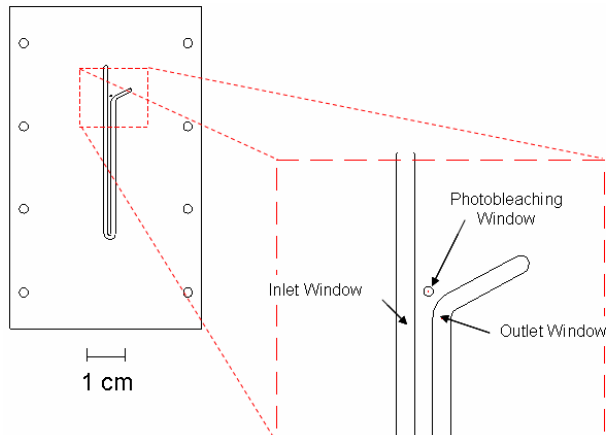
The device design in Fig. 1 creates one additional complication for applying this method: there is a tapered change in cross-section. To account for this change, the taper was modeled simply: half of its length was considered to be narrow channel, and half was considered to be wide channel. Each section of channel was treated as a separate element that introduced its own dispersion, and variances of each of the three sections (narrow, wide, narrow) were added, a common

practice in chromatography.³ The difference in centerline velocity was also accounted for in each section.

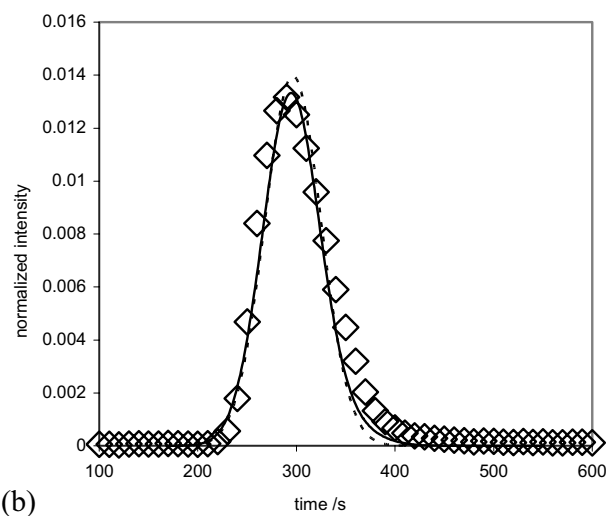
The predicted peaks were calculated and compared to experimental data (not shown). Although the magnitude of dispersion is predicted reasonably well, the predicted peaks differ from the observed results for negative controls in two important ways: 1) The peak predictions are always completely symmetrical, because of the underlying Gaussian character. This is not observed for the negative control peaks. Asymmetry can result from elements in the fluidic circuit that produce undesirable mixing.³ These can be as simple as an abrupt change in cross-sectional area (which motivated the tapered channel sections), especially if an increase in cross-sectional area is rapidly followed by a decrease. It should be emphasized that the inlet peaks are not symmetric either, so even if the dispersion in the channel is Gaussian, the outlet peaks will remain asymmetric on the time-scale considered. The fluidic interface comprising the round inlet tubing, the round inlet hole, and the rectangular channel seems like the most likely location for an upstream mixing element. 2) The calculations suggest that the peak centroids should be moving faster than they are. This could be the result of incorrectly accounting for the tapered section of the channel. This could also be caused by an unintended mixing element³, as these features can act as “fluid capacitors”.

We hypothesized that the tapered channel and an unidentified upstream unintended mixing element were responsible for the discord between our observations and the predictions of the simple Taylor model. The device was redesigned to be as simple as possible; i.e., no changes in channel cross-section between inlet and outlet, and only one turn of the largest radius possible (Supplementary Material Fig. 3a). The inlet peaks were also convoluted with a discrete Gaussian of the expected variance (from Equation 4) using Matlab; i.e., the $f_i(t_i)$ of Equation 3 constituted the vectors of inlet values. The outlet peaks resulting from this second generation device match the analytical predictions well, and the convolution with the inlet matches more closely than a symmetrical Gaussian-spread plug (Supplementary Material Fig. 3b).

The results gathered on the first generation device are still valid; however, future investigation will use the redesigned device to enable the simple analytical prediction of the negative result.



(a)



(b)

Supplementary Material, Fig. 3 a) The revised channel design eliminates the changes in cross-sectional area and the tapered section, and eliminates unnecessary turns. b) A representative comparison of the observed outlet peaks for fluorescein to predictions for a negative control from a simple Taylor dispersion model with the revised design. (—) = prediction as described in text, (---) = simple Gaussian-spread plug, (○) = observed outlet points. Symbol size corresponds to error bars. Observations are the mean of all five runs (not shown elsewhere) and the corresponding values for parameters in the Taylor model have been used.

Notes and references

- ¹⁴⁵ 1. G. Taylor, *Proceedings of the Royal Society of London. Series A, Mathematical and Physical Sciences*, 1954, **225**, 473-477.
- 2. G. Taylor, *Proceedings of the Royal Society of London. Series A, Mathematical and Physical Sciences*, 1953, **219**, 186-203.
- 3. J. C. Sternberg, in *Advances in chromatography*, eds. J. C. Giddings and R. A. Keller, Marcel Dekker,, New York,, Editon edn., 1966, , vol. 2, pp. 205-269.
- 4. R. Aris, *Proceedings of the Royal Society of London. Series A, Mathematical and Physical Sciences*, 1959, **252**, 538-550.
- 5. S. Ghosal, *Journal of Fluid Mechanics*, 2002, **459**, 103-128.